MCB
Journals.ASM.org

High CO_2 Leads to Na,K-ATPase Endocytosis via c-Jun Amino-Terminal Kinase-Induced LMO7b Phosphorylation

Laura A. Dada,[a] Humberto E. Trejo Bittar,[a] Lynn C. Welch,[a] Olga Vagin,[b] Nimrod Deiss-Yehiely,[a] Aileen M. Kelly,[a]* Mairead R. Baker,[a] Joseph Capri,[c] Whitaker Cohn,[c] Julian P. Whitelegge,[c] István Vadász,[a,d] Yosef Gruenbaum,[a,e] Jacob I. Sznajder[a]

Division of Pulmonary and Critical Care Medicine, Feinberg School of Medicine, Northwestern University, Chicago, Illinois, USA[a]; Department of Physiology, UCLA, and Veterans Affairs, Greater Los Angeles Healthcare System, Los Angeles, California, USA[b]; The NPI-Semel Institute, Pasarow Mass Spectrometry Laboratory, UCLA, Los Angeles, California, USA[c]; Department of Internal Medicine, Justus Liebig University, Universities of Giessen and Marburg Lung Center, Giessen, Germany[d]; The Alexander Silberman Institute of Life Sciences, Edmond Safra Campus, The Hebrew University of Jerusalem, Jerusalem, Israel[e]

The c-Jun amino-terminal kinase (JNK) plays a role in inflammation, proliferation, apoptosis, and cell adhesion and cell migration by phosphorylating paxillin and β-catenin. JNK phosphorylation downstream of AMP-activated protein kinase (AMPK) activation is required for high CO_2 (hypercapnia)-induced Na,K-ATPase endocytosis in alveolar epithelial cells. Here, we provide evidence that during hypercapnia, JNK promotes the phosphorylation of LMO7b, a scaffolding protein, *in vitro* and in intact cells. LMO7b phosphorylation was blocked by exposing the cells to the JNK inhibitor SP600125 and by infecting cells with dominant-negative JNK or AMPK adenovirus. The knockdown of the endogenous LMO7b or overexpression of mutated LMO7b with alanine substitutions of five potential JNK phosphorylation sites (LMO7b-5SA) or only Ser-1295 rescued both LMO7b phosphorylation and the hypercapnia-induced Na,K-ATPase endocytosis. Moreover, high CO_2 promoted the colocalization and interaction of LMO7b and the Na,K-ATPase α_1 subunit at the plasma membrane, which were prevented by SP600125 or by transfecting cells with LMO7b-5SA. Collectively, our data suggest that hypercapnia leads to JNK-induced LMO7b phosphorylation at Ser-1295, which facilitates the interaction of LMO7b with Na,K-ATPase at the plasma membrane promoting the endocytosis of Na,K-ATPase in alveolar epithelial cells.

Patients with acute respiratory distress syndrome and chronic obstructive pulmonary disease can develop elevated levels of CO_2 in blood and tissue (hypercapnia), which is associated with worse outcomes (1–4). Recent studies demonstrated that high CO_2 levels impair alveolar edema clearance, an important function of the alveolar epithelium (3, 5–7). The clearance of alveolar edema is effected by active Na^+ transport via the apical Na^+ channels and the basolateral Na,K-ATPase (8–12).

Na,K-ATPase is a transmembrane protein comprised of a catalytic α subunit and a structural β subunit (13) and is localized on the basolateral surface of mammalian epithelial cells. Endocytosis has been shown to reduce Na,K-ATPase for both enzymatic activity and lung edema clearance (7, 10, 14–16). We have previously reported that hypercapnia leads to the endocytosis of Na,K-ATPase via a mechanism that involves the activation of 5′ AMP-activated protein kinase (AMPK) and protein kinase Cζ (PKCζ) (5, 7, 17). More recently, we demonstrated that c-Jun N-terminal kinase (JNK) is activated during hypercapnia and leads to the endocytosis of the Na,K-ATPase (6). However, the mechanisms by which JNK promotes Na,K-ATPase endocytosis still are unclear. JNK is a serine/threonine protein kinase, belonging to a group of mitogen-activated protein kinases (MAPK), which, upon activation by extracellular stimuli, regulates cellular responses leading to cell adaptation, survival, or apoptosis (18). The majority of the substrates for JNK are transcription factors and antiapoptotic proteins (19, 20). However, JNK also participates in actin reorganization and remodeling (21, 22) and has been implicated in the regulation of cell-cell adhesion by phosphorylating β-catenin, triggering its endocytosis (23, 24). An important feature of the MAPK signaling pathways is the formation of signaling complexes that contain not only active kinases but also scaffold proteins that lack enzymatic activity. It has been proposed that the phosphorylation of scaffolding proteins regulates interactions with their binding partners (19, 25). To assess potential targets of JNK regulating Na,K-ATPase endocytosis during hypercapnia, we performed a screen with an antibody that recognizes proteins phosphorylated in a MAPK consensus sequence (a phosphorylated serine or threonine residue followed by a proline residue [26]) and identified LIM domain-only 7b (LMO7b), a protein that has been described to regulate the actin cytoskeleton in epithelial cells (27, 28). LMO7b contains PDZ and LIM domains that are involved in protein-protein interactions and the calponin homology domain, which binds actin (27). Here, we report that hypercapnia induces the phosphorylation of LMO7b downstream of JNK, which facilitates the interaction of LMO7 with Na,K-ATPase at the plasma membrane and leads to Na,K-ATPase endocytosis in alveolar epithelial cells.

Received 20 August 2015 **Accepted** 9 September 2015

Accepted manuscript posted online 14 September 2015

Citation Dada LA, Trejo Bittar HE, Welch LC, Vagin O, Deiss-Yehiely N, Kelly AM, Baker MR, Capri J, Cohn W, Whitelegge JP, Vadász I, Gruenbaum Y, Sznajder JI. 2015. High CO_2 leads to Na,K-ATPase endocytosis via c-Jun amino-terminal kinase-induced LMO7b phosphorylation. Mol Cell Biol 35:3962–3973. doi:10.1128/MCB.00813-15.

Address correspondence to Laura A. Dada, Lauradada@northwestern.edu.

L.A.D. and H.E.T.B. contributed equally to the manuscript.

* Present address: Aileen M. Kelly, Department of Molecular and Cell Biology, University of California, Berkeley, Berkeley, California, USA.

MATERIALS AND METHODS

Reagents. All chemical reagents were purchased from Sigma-Aldrich (St. Louis, MO) unless stated otherwise. Ouabain was purchased from ICN Biomedicals Inc. (Aurora, OH). All cell culture reagents were obtained from Corning Life Sciences (Tewksbury, MA). Normal goat serum was purchased from Jackson ImmunoResearch Laboratories, Inc. (West Grove, PA). The following antibodies and other reagents were used in this study: LMO7 863 (28) (a gift from Jun Miyoshi, Osaka Medical Center for Cancer and Cardiovascular Diseases, Osaka, Japan), LMO7 M-300 and green fluorescent protein (GFP) monoclonal antibodies (Santa Cruz Biotechnology Inc., Santa Cruz, CA), phosphothreonine/serine-proline (pT/S-P) and phospho-MAPK—cyclin-dependent kinase substrate (pMAPK) (Cell Signaling Technology, Danvers, MA), Na,K-ATPase-α_1 subunit from EMD Millipore (Billerica, MA), mouse antihemagglutinin (anti-HA) (Covance, Princeton, NJ), GFP polyclonal antibody (Clontech, Palo Alto, CA), mouse anti-FLAG-M2 (Sigma-Aldrich), Alexa Fluor 488 and 568 (Life Technologies, Grand Island, NY), secondary goat anti-mouse antibody–horseradish peroxidase (HRP), and goat anti-rabbit antibody–HRP (Bio-Rad, Hercules, CA). Recombinant active JNK1 was from Signal Chem (Richmond, BC, Canada). [γ-^{32}P]ATP was purchased from PerkinElmer Life Sciences (Waltham, MA). Protein A/G Plus-agarose beads were from Santa Cruz Biotechnology Inc. Lipofectamine 2000 and Lipofectamine RNAiMax were purchased from Life Technologies. pCMV-FLAG-LMO7b, which expresses the FLAG-tagged full-length rat FLAG-LMO7b, was kindly provided by Y. Takai (Kobe University Graduate School of Medicine, Kobe, Japan). The initial mass spectrometry (MS) analysis and the determination of phospho sites in LMO7b were performed at the Taplin Mass Spectrometry Facility (Harvard Medical School, Boston, MA).

Alveolar epithelial cell isolation and culture. Animals were provided with food and water *ad libitum*, maintained on a 14-h:10-h light-dark cycle, and handled according to National Institutes of Health guidelines and the Northwestern University Institutional Animal Care and Use Committee-approved experimental protocol. Alveolar epithelial type II (rATII) cells were isolated from the lungs of Sprague-Dawley rats (200 to 225 g) by elastase digestion, as previously described (29). The day of isolation and plating was designated culture day 0. All experiments were conducted on day 2 or 3. Human A549 cells (ATCC CCL 185; Manassas, VA) or A549 cells stably expressing the rat Na,K-ATPase-α_1 subunit tagged with GFP (A549-GFP-α_1) were previously described (10). A549-GFP-α_1 cells show the same enzymatic activity and respond to stimuli similarly to wild-type (WT) A549 cells (30). Cells were grown in Dulbecco's modified Eagle medium (DMEM) supplemented with 10% fetal bovine serum (FBS), 100 U/ml penicillin, and 100 μg/ml streptomycin. For A549-GFP-α_1, 3 μM ouabain was added to suppress the endogenous Na,K-ATPase-α_1 subunit. Cells were incubated in a humidified atmosphere of 5% CO_2 and 95% air at 37°C.

CO_2 media and CO_2 exposure. For the different experimental conditions, initial solutions were prepared with DMEM–Ham's F-12 medium-Tris base (3:1:0.5) containing 10% fetal bovine serum with 100 U/ml penicillin and 100 μg/ml streptomycin. The buffering capacity of the media was modified by changing its initial pH with Tris base in order to obtain pH 7.4 at the various CO_2 levels (partial CO_2 pressure [pCO_2] of 40, 60, 80, and 120 mm Hg) (4). The desired CO_2 and pH levels were achieved by equilibrating the media overnight in a humidified chamber (C-chamber; BioSpherix Ltd., Lacona, NY). The C-chamber's atmosphere was controlled with a PRO-CO_2 carbon dioxide controller (Biospherix). In this chamber, cells were exposed to the desired pCO_2 while maintaining 21% O_2 balanced with N_2. Prior to and after CO_2 exposure, pH, pCO_2, and pO_2 levels in the media were measured using a Stat Profile pHOx blood gas analyzer (Nova Biomedical, Waltham, MA). Experiments were started by replacing culture media with the CO_2-equilibrated media and incubating in the C-chamber for the desired time. Normoxic conditions were consistent over the course of all experiments.

Generation of LMO7b mutants. The different rat FLAG-LMO7b mutants were created by replacing the serine residues in the indicated positions with alanine residues using the QuikChange XL site-directed mutagenesis kit (Stratagene, La Jolla, CA) by following the manufacturer's protocols for primer design and reaction conditions. Rat FLAG-LMO7b-WT was used as the template, from which subsequent point mutations were performed in separate reactions. The following mutants were generated using the corresponding template and primers: for FLAG-LMO7b-S727A (WT-FLAG-LMO7b), 5′-GAGGGAAGTTTCAAGGGCCCCGGATCAGTTCAG-3′ and 5′-CTGAACTGATCCGGGGCCCTTGAAACTTCCCTC-3′; FLAG-LMO7b-S1295A (WT-FLAG-LMO7b), 5′-CTCAGTGAAGACCGCCCCGGGGTCTCC-3′ and 5′-GGAGACCCCGGGGCGGTCTTCACTGAG-3′; FLAG-LMO7b-S1305A (WT-FLAG-LMO7b), 5′-TCCCTCTCCACGTAGCCATGCTCCTTCGATG-3′ and 5′-CATCGAA GGAGCATGGCTACGTGGAGAGGGA-3′; FLAG-LMO7b-S727-1295A (FLAG-LMO7b-S727A), 5′-CTCAGTGAAGACCGCCCCGGGGTCTCC-3′ and 5′-GGAGACCCCGGGGCGGTCTTCACTGAG-3′; FLAG-LMO7b-S727-1305A (FLAG-LMO7b-S727A), 5′-TCCCTCTCCACGTAGCCATGCTCCTTCGATG-3′ and 5′-CATCGAAGGAGCATGGCTACGTGGAGAGGGA-3′; FLAG-LMO7b-3SA (S727, 1295, 1305A) (FLAG-LMO7b-S727-1305A), 5′-CTCAGTGAAGACCGCCCCGGGGTCTCC-3′ and 5′-GGAGACCCCGGGGCGGTCTTCACTGAG-3′; FLAG-LMO7b-4SA (S727, 1295, 1300, 1305A) (FLAG-LMO7b-3SA), 5′-CCGGGGTCTCCCGCTCCACGTAGCC-3′ and 5′-GGCTACGTGGAGCGGGAGACCCCGG-3′; FLAG-LMO7b-5SA (S727, 1295, 1298, 1300, 1305A) (FLAG-LMO7b-4SA), 5′-GTGAAGACCGCCCCGGGGGCTCCCGCTCCACGTA-3′ and 5′-TACGTGGAGCGGGAGCCCCCGGGGCGGTCTTCAC-3′. The mutations were verified by traditional DNA sequencing performed at the Northwestern University Genomics Core Facility.

Immunoprecipitation. Either rATII cells (day 2 postisolation) or A549 cells were used. When A549 cells were used, cells were transiently transfected either with FLAG-LMO7b-WT or FLAG-LMO7b-5SA mutants. Cells were exposed to 40 or 120 mm Hg CO_2 at 37°C for 10 min, placed on ice, and washed twice with ice-cold PBS. Cell were lysed in a buffer containing 150 mM NaCl, 50 mM Tris, 1% Triton X-100, 1 mM EGTA, 1 mM EDTA, 2.5 mM sodium pyrophosphate, 1 mM β-glycerophosphate, 1 mM NaF, 1 mM Na_3VO_4, 1 mM phenylmethylsulfonyl fluoride (PMSF), 100 μg/ml *N-p*-tosyl-L-phenylalanine chloromethyl ketone (TPCK), and 1 μg/ml leupeptin. LMO7 was immunoprecipitated by incubating equal amounts of protein (1,000 μg) with 2 μl of LMO7 863, 20 μl of LMO7 M-300 (for the endogenous protein), or 2 μl of FLAG antibodies and 40 μl of Protein A/G Plus-agarose beads for 2 h at 4°C. The immune complexes were washed three times with lysis buffer, resuspended in 2× Laemmli sample buffer, and analyzed by SDS-PAGE and Western blotting.

Western blot analysis. Protein was quantified by Bradford assay (Bio-Rad, Hercules, CA) (31) and resolved in 7.5 to 12.5% polyacrylamide gels (SDS-PAGE). Thereafter, proteins were transferred onto nitrocellulose membranes (GE Healthcare Life Sciences, Pittsburgh, PA) using a semi-dry transfer apparatus (Bio-Rad). Incubation with specific antibodies was performed overnight at 4°C. When more than one primary antibody was used on the same membrane, blots were stripped by incubating for 1 h at 55°C in stripping solution (62.5 mM Tris-HCl, 2% SDS, 100 mM 2-mercaptoethanol, pH 6.8). Blots were developed with a chemiluminescence detection kit (PerkinElmer Life Sciences) used as recommended by the manufacturer. The band's signals in the linear range were quantified by densitometric scan (ImageJ 1.46r; National Institutes of Health, Bethesda, MD).

Adenoviral infection of ATII cells. Day 2 rATII cells, plated on 100-mm cell culture dishes, were incubated with adenovirus-null (Ad-null; 20 PFU/cell) or with an adenovirus kinase-dead (K45R) variant of the AMPK-α_1 subunit tagged with HA (Ad-DN-AMPK) (7, 32) or with an adenovirus expressing a dominant-negative JNK1 tagged with GFP (Ad-DN-JNK) (7) for 4 h in 4 ml DMEM as we previously described (3, 7).

After the incubation, medium was supplemented with 10% fetal bovine serum, 100 U/ml penicillin, and 100 μg/ml streptomycin, and experiments were performed 24 h later.

***In vitro* kinase assay.** For endogenous LMO7b experiments, day 2 postisolation rATII cells were used. When FLAG-LMO7b was used as the substrate, A549 cells were transiently transfected either with FLAG-LMO7b-WT or with FLAG-LMO7b serine-to-alanine mutants by using Lipofectamine 2000 as described by the manufacturer, and cells were used after 48 h. Cell lysates were obtained, and LMO7b was immunoprecipitated by incubating ~1,000 μg of protein with either 20 μl of LMO7 M-300 antibody or 3 μl of FLAG antibody in lysis buffer overnight. Immunoprecipitated LMO7b was incubated with a mixture containing 150 ng of recombinant active mouse JNK1 protein, 5 μCi [γ-^{32}P]ATP, and 100 μM ATP for 40 min at 30°C in a solution of 25 mM Tris-HCl (pH 7.5), 5 mM β-glycerophosphate, 2 mM dithiothreitol (DTT), 0.1 mM Na_3VO_4, 10 mM $MgCl_2$ (pH 7.5). The reactions were stopped by cooling the samples on ice and adding Laemmli sample buffer. The proteins were separated by SDS-PAGE, and radiolabeled LMO7b was detected by autoradiography.

Transfection of A549 cells with siRNA. A549 cells were plated in 60-mm cell culture dishes and transfected with 120 pmol of human LMO7 short interfering RNA (siRNA) duplex (final concentration, 100 μM) (Santa Cruz Biotechnology, Santa Cruz, CA) using Lipofectamine RNAiMAX as recommended by the manufacturer, and experiments were performed 48 h later. A nonsilencing negative-control siRNA was purchased from Life Technologies.

Cell surface biotinylation. A549 cells were transiently transfected either with FLAG-LMO7b-WT or with the different FLAG-LMO7b serine-to-alanine mutants using Lipofectamine 2000, as described by the manufacturer; experiments were performed 48 h after transfection. Cells were exposed to 40 or 120 mm Hg CO_2 at 37°C for 30 min. Cell surface proteins were labeled for 20 min using 1 mg/ml EZ-Link *N*-hydroxysuccinimide-SS-biotin (Thermo Scientific Pierce Protein Biology, Rockford, IL) as we previously described (6, 7). After cell lysis, samples containing 150 μg of protein were incubated overnight at 4°C with end-over-end shaking in the presence of streptavidin beads (Thermo Scientific Pierce Protein Biology) and analyzed by SDS-PAGE and Western blotting, as described previously (10).

Immunofluorescence confocal microscopy. rATII or A549-GFP-α_1 cells were allowed to grow on coverslips. After 15 min of CO_2 exposure, cells were washed three times with PBS, fixed in 3.7% formaldehyde in PBS, blocked with goat serum, and immunostained with anti-LMO7b 863 (1:500) and Na,K-ATPase-α_1 (1:100) in blocking solution for 1 h. Secondary antibodies were diluted 1:100 in blocking solution and incubated for 1 h. For some experiments, cells were preincubated with SP600125 (20 μM) for 30 min before the experiment and during CO_2 exposure. Images were obtained using a Zeiss LSM 510 laser-scanning confocal microscope using a Plan Apochromat, ×63, 1.4-numeric-aperture oil objective (Zeiss, Heidelberg, Germany). Contrast and brightness settings were adjusted so that all pixels were in the linear range. The coefficient of colocalization of Na,K-ATPase α_1 subunit with LMO7b (means ± standard errors of the means [SEM]) was calculated by using ZEN 2009 software (Carl Zeiss MicroImaging GmbH, Germany) as previously described (33). Imaging work was performed at the Northwestern University Center for Advanced Microscopy (Cell Imaging Facility and Nikon Imaging Center), which was generously supported by NCI CCSG P30 CA060553, awarded to the Robert H. Lurie Comprehensive Cancer Center.

Coimmunoprecipitation. A549-GFP-α_1 cells were transiently transfected with either FLAG-LMO7b-WT or 5SA as described above. Cells were exposed to 40 or 120 mm Hg CO_2 at 37°C for 15 min. In some experiments, cells were preincubated with SP600125 (20 μM) for 30 min. Cells were placed on ice and washed twice with ice-cold PBS before being homogenized for 30 min in a low-detergent lysis buffer containing 150 mM NaCl, 20 mM HEPES, 0.1% NP-40, 5% (vol/vol) glycerol, 2 mM EGTA, 2 mM EDTA, 1 mM NaF, 1 mM Na_3VO_4, 1 mM PMSF, 100 μg/ml TPCK, and 1 μg/ml leupeptin (pH 7.4) (16). The cell extract was obtained by centrifugation at 18,000 × *g* for 15 min. Equal amounts of protein (1,000 μg) then were incubated with 3 μl of GFP polyclonal antibody and 40 μl of Protein A/G Plus-agarose beads (Santa Cruz Biotechnology) overnight at 4°C. The immune complexes were washed three times with lysis buffer, resuspended in 2× Laemmli sample buffer, and analyzed by SDS-PAGE and Western blotting.

Protein digestion, isotopic labeling, liquid chromatography (LC), and mass spectrometry. To analyze the proteins that coimmunoprecipitate with LMO7b, rATII cells were exposed to normocapnia and hypercapnia, lysed with a low-detergent buffer, and immunoprecipitated with the LMO7b M300 antibody as described above. Immunoprecipitated proteins were reduced with 5 mM tris(2-carboxyethyl)phosphine (final concentration) for 30 min at room temperature and subsequently alkylated with 10 mM iodoacetamide (final concentration) for 30 min at room temperature in the dark. Samples then were diluted 1:5 (vol/vol) with 50 mM triethylammonium bicarbonate and enzymatically digested with trypsin overnight at 1:50 (wt/wt) enzyme-protein at 37°C. Sodium deoxycholate was precipitated out of solution with 0.5% trifluoroacetic acid (final concentration), phase transferred in 1:1 (vol/vol) ethyl acetate, and centrifuged at 16,000 × *g*. The organic phase was aspirated and the peptides were lyophilized. In-solution dimethyl labeling was performed according to Boersema et al. (34), and labeled peptides were combined 1:1 (wt/wt). Strong cation exchange and desalting of the samples was executed via StageTipssilber (35). Fractionated samples were analyzed with an Eksigent two-dimensional NanoLC (nLC) attached to a Thermo Orbitrap XL. Peptides were injected onto a laser-pulled nanobore 20-cm by 75-μm C_{18} column (Acutech Scientific) in buffer A (3% acetonitrile with 0.1% formic acid) and resolved using a 3-h linear gradient from 3 to 40% buffer B (100% acetonitrile with 0.1% formic acid). The Orbitrap XL was operated in data-dependent mode with 60,000 resolution and target autogain control at 5e6 for parent scan. The top 12 ions above a charge of +1 were subjected to collision-induced dissociation set to a value of 35 with target autogain control of 5,000. Dynamic exclusion was set to 30 s. Raw data were processed and quantified using Sequest and Thermo Proteome Discoverer (v1.4). The Uniprot mouse database was searched with variable modifications of methionine oxidation, fixed modification of cysteine carbamidomethylation, 2 missed cleavages by trypsin, and allowing 10 ppm and 0.5-Da mass error on the full MS and tandem MS (MS/MS), respectively. Peptides and proteins were filtered using Percolator with a 1% false discovery rate.

Statistical analysis. Data are presented as means ± SEM and were analyzed statistically using one-way analysis of variance, followed by a multiple comparison with Dunnett's test. A P value ≤0.05 was considered statistically significant.

RESULTS

Hypercapnia-induced LMO7b phosphorylation is dependent of JNK activation. We have previously reported that exposing rATII or A549 cells to elevated CO_2 levels resulted in a concentration-dependent decrease in the Na,K-ATPase-α_1 subunit protein abundance at the plasma membrane (5). High CO_2 also led to time- and concentration-dependent JNK activation, which was required for hypercapnia-induced Na,K-ATPase endocytosis (6). While it has been described that Na,K-ATPase-α_1 is phosphorylated by ERK1/2 (36, 37), our previous report suggested that JNK does not directly phosphorylate the Na,K-ATPase-α_1 subunit (6). To identify a target of JNK phosphorylation during hypercapnia in the alveolar epithelium, rATII cells were exposed to high CO_2 for 10 min and analyzed for the presence of phosphorylated proteins by Western blotting using a pT/S-P antibody (26). Among several bands, the one at ~150 kDa was observed only in the absence of the competitive inhibitor of JNK phosphorylation, SP600125. Mass spectrometry analysis revealed that the observed

A

LMO7b, gi|46811858, MWt 156553, Protein Score 43

Peptide sequence	Calc. Mass	Obsrv. Mass	± da	± ppm
LREEWQR	1016.5272	1016.5306	0.0034	3
QQILQEMR	1045.5459	1045.5415	-0.0044	-4
ARAHPAEMPK	1123.5677	1123.6597	0.092	82
GDFPAPPGSHR	1137.5436	1137.6354	0.0918	81
EPICLTGIMR	1148.5802	1148.6074	0.0272	24
EQDRLLQEK	1158.6113	1158.5884	-0.0229	-20
QQILQEMRK	1173.6409	1173.67	0.0291	25
VCSYCNSILGK	1186.5594	1186.5557	-0.0037	-3
YSDRIGTTSFSQR	1517.7343	1517.7654	0.0311	20
GQLEDDAVYEDQSQK	1724.761	1724.8861	0.1251	73
SASVNKEPICLTGIMR	1734.8877	1734.9106	0.0229	13
AAGMKPDSSHFILGSSSEK	1964.9382	1964.9156	-0.0226	-12

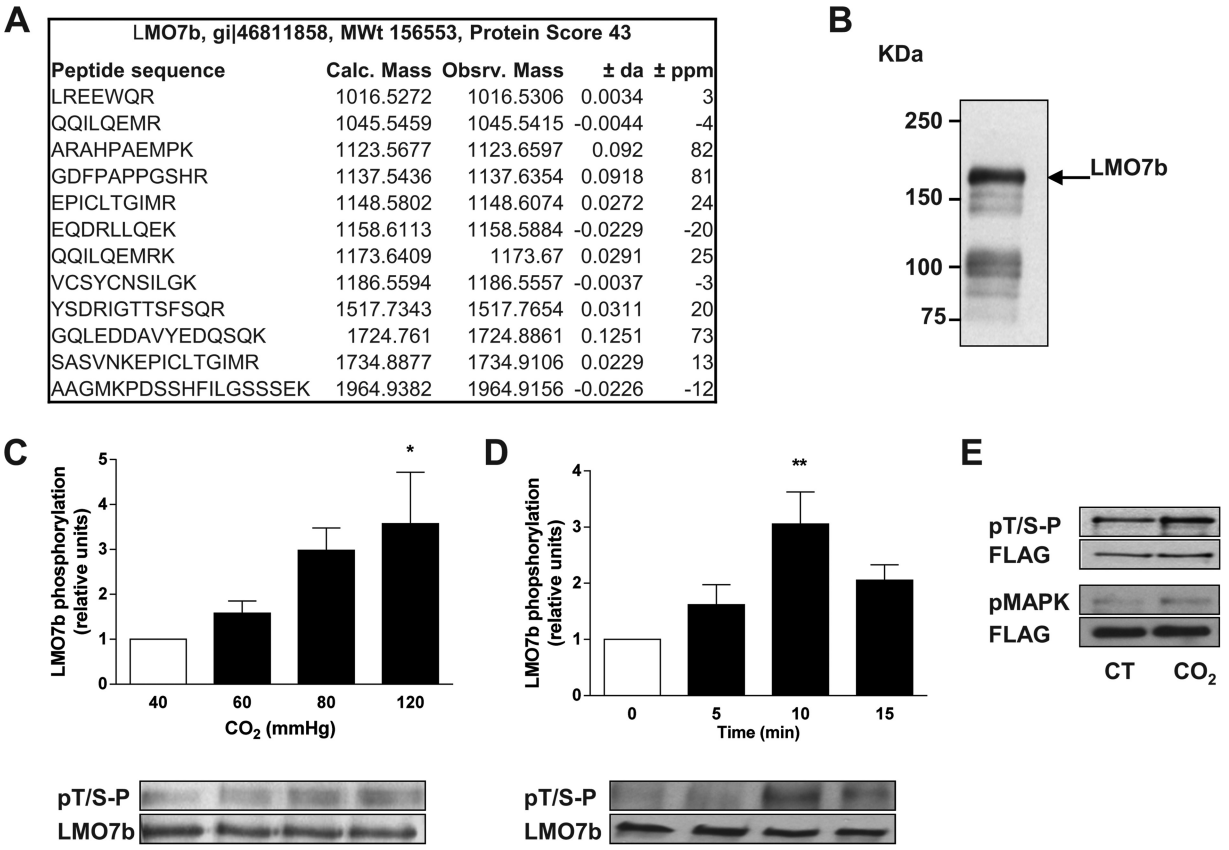

FIG 1 LMO7b is phosphorylated during hypercapnia in T/S-P domain. (A) rATII cells were exposed to 120 mm Hg CO_2 for 10 min in the presence or absence of the inhibitor of JNK phosphorylation, SP600125, and analyzed by Western blotting (WB) using a pT/S-P antibody. A band at ~150 kDa was detected only in the absence of SP600125. The nLC MS/MS analysis of the band at ~150 kDa excised from a parallel gel identified peptides corresponding to rat LMO7b. Calc., calculated; Obsrv., observed. (B) Expression of LMO7b isoforms in isolated rATII cells. (C) rATII cells were exposed for 10 min to either normocapnia (40 mm Hg CO_2) or increasing concentrations of CO_2. LMO7b was immunoprecipitated, and phosphorylation was assessed using a pT/S-P by WB. Immunoprecipitated LMO7b was used as a loading control. Results are means ± SEM; $n = 3$. (D) rATII cells were exposed to hypercapnia (120 mm Hg CO_2) for the indicated times. Samples were processed as described for panel C. Results are means ± SEM; $n = 3$. (E) A549 cells expressing rat FLAG-LMO7b were exposed to 40 mm Hg CO_2 (CT) or 120 mm Hg CO_2 (CO_2) for 10 min. LMO7b was immunoprecipitated using a FLAG antibody. Phosphorylation was assessed by WB using a pT/S-P or a pMAPK substrate (pMAPK) antibody. FLAG was used as a loading control. *, $P < 0.05$; **, $P < 0.01$.

phosphorylated band corresponds to the rat LMO7b (Fig. 1A). Rat LMO7 is expressed as two splice variants, LMO7a (196 kDa) and LMO7b (157 kDa) (27); however, rATII cells only express LMO7b (Fig. 1B), which is consistent with a previous report on adult mouse lung (28). Also, in agreement with the previous report in rodent lungs, the polyclonal antibody used recognized faster-migrating bands (28). Little is known about the regulation of LMO7b function, and no phosphorylation sites have been described. To study LMO7b phosphorylation, rATII cells were exposed to high CO_2, and the phosphorylation of immunoprecipitated LMO7b was assessed by Western blotting with pT/S-P. Hypercapnia increased LMO7b phosphorylation in a concentration-dependent mode (Fig. 1C). At 120 mm Hg of CO_2, maximal phosphorylation was achieved after 10 min of exposure (Fig. 1D). All subsequent experiments to study LMO7b phosphorylation were carried out at 120 mm Hg of CO_2 for 10 min unless otherwise stated. In A549 cells transfected with rat FLAG-LMO7b, high CO_2 increased LMO7b phosphorylation, as assessed by Western blotting using pT/S-P or phospho-MAPK substrate antibodies (Fig. 1E).

To determine whether LMO7 was phosphorylated via a JNK-dependent pathway, rATII cells were pretreated with SP600125 or infected with Ad-DN-JNK (6). Both treatments inhibited the CO_2-increased LMO7b phosphorylation compared to that with a vehicle or Ad-null infection (Fig. 2A and B). We have previously reported that during hypercapnia, AMPK-dependent phosphorylation was required for both JNK activation and Na,K-ATPase endocytosis (6, 7). In agreement with those results, the infection of rATII cells with Ad-DN-AMPK also prevented LMO7b phosphorylation induced by CO_2 (Fig. 2C). Taken together, these data suggest that the CO_2-induced LMO7b phosphorylation in a T/S-P domain is dependent on JNK activity.

JNK phosphorylates LMO7 *in vitro*. Subsequently, we investigated whether JNK phosphorylates LMO7b. We performed an *in vitro* kinase assay using LMO7b, which was immunoprecipitated from rATII cells, as a substrate and a commercially available recombinant active JNK1. Under these conditions, JNK phosphorylated LMO7b (Fig. 3A). Interestingly, we observed some phosphorylation of LMO7b even in the absence of the kinase, and a similar result was obtained when we used FLAG-LMO7b as a substrate, suggesting that other kinases are present (Fig. 3B). The presence of SP600125 in the assay prevented the increase in LMO7b phosphorylation induced by JNK (Fig. 3C), and the phos-

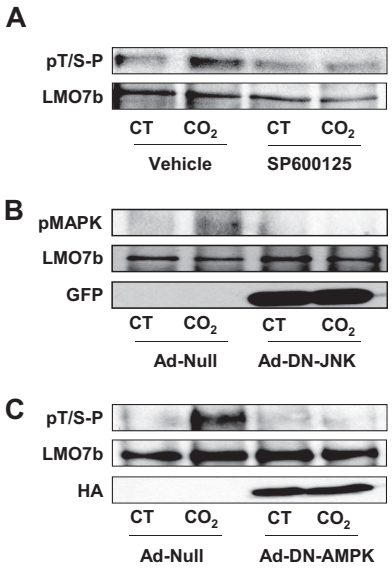

FIG 2 LMO7b is phosphorylated during hypercapnia downstream of AMPK and JNK. (A) rATII cells were pretreated with SP600125 (20 μM for 30 min) and then exposed to normocapnia (CT) or hypercapnia (CO_2) for 10 min. LMO7b was immunoprecipitated and phosphorylation assessed by WB with a pT/S-P antibody. Immunoprecipitated LMO7b is shown as a loading control. (B and C) rATII cells were infected with a null adenovirus (Ad-null) or an adenovirus expressing DN-JNK and GFP (B) or with Ad-null or Ad-DN-HA-AMPK (C). After 24 h, cells were exposed to CO_2 and processed as described for panel A, and WB were developed with a pMAPK (B) or with a pT/S-P antibody (C). GFP and HA Western blots are shown as markers of infection. $n = 3$.

phorylated band observed in the absence of added exogenous kinase was not affected by the presence of SP600125 in the assay. These results indicate that LMO7b is an *in vitro* substrate for JNK, although we cannot exclude the presence of another kinase that was coimmunoprecipitated with LMO7b and activated by JNK during the kinase assay.

We next sought to determine the residues of LMO7b that are phosphorylated by JNK. For this purpose, we used mass spectrometry to map serine and threonine phosphorylation sites in LMO7b samples from cells exposed to 40 or 120 mm Hg CO_2 and found seven peptides which were assigned as phosphorylation sites. However, none were differentially phosphorylated during hypercapnia compared to that during normocapnia, which is consistent with the data in Fig. 1 and 2 showing that LMO7b has a basal level of phosphorylation. Out of the phosphorylated peptides, we choose those in which the phosphorylated Ser/Thr was followed by a Pro and identified the presence of five potential JNK phosphorylation sites: Ser-727, Ser-1295, Ser-1298, Ser-1300, and Ser-1305 (Fig. 3D). Interestingly, using Scansite3 and Kinephos 2.0, we found that Ser-727, Ser-1295, Ser-1298, Ser-1300, and Ser-1305 are predicted phosphorylation sites of the CMCG kinases, of which the MAPK family is a subgroup (19). We mutated the five potential JNK phosphorylation sites in FLAG-LMO7b to alanine (FLAG-LMO7b-5SA) by site-directed mutagenesis. The *in vitro* kinase assay showed that FLAG-LMO7b-5SA was not phosphorylated by the active JNK1, in contrast to FLAG-LMO7b-WT (Fig. 3E). We next analyzed whether LMO7b also was phosphorylated in those sites in intact cells. A549 cells were transfected with FLAG-LMO7b-WT or FLAG-LMO7b-5SA and exposed to high CO_2. The replacement of the five serine residues by alanine residues resulted in a significant reduction in phosphorylation compared to the level with WT LMO7b (Fig. 3F). Collectively, these results indicate that during hypercapnia LMO7b is phosphorylated both *in vitro* and *in vivo* downstream of JNK activation.

JNK-dependent LMO7b phosphorylation is required for hypercapnia-mediated Na,K-ATPase endocytosis. To study whether LMO7b plays a role in hypercapnia-induced Na,K-ATPase endocytosis, we silenced LMO7b. This treatment prevented the hypercapnia-induced decrease of the α_1 subunit in the plasma membrane in A549 cells (Fig. 4A). We next studied the functional consequences of CO_2-induced LMO7b phosphorylation on the endocytosis of the Na,K-ATPase. We generated several mutants where the potential JNK phosphorylation sites in LMO7b were replaced by alanine residues individually or in combination. Besides the LMO7b-5SA construct, we generated FLAG-LMO7b-4SA (S727A,S1295A, S1300A,S1305A), FLAG-LMO7b-3SA (S727A,S1295A,S1305A), FLAG-LMO7b-S727A,S1305A, FLAG-LMO7b-S727A,S1295A, FLAG-LMO7b-S727A, and FLAG-LMO7b-S1295A (Fig. 4B). The expression of FLAG-LMO7b-5SA, FLAG-LMO7b-4SA, or FLAG-LMO7b-3SA prevented hypercapnia-induced Na,K-ATPase endocytosis, excluding a role for S1300 and S1298 as phosphorylation targets of JNK-induced phosphorylation (Fig. 4C). Interestingly, the expression of FLAG-LMO7b-S727A,S1305A did not prevent endocytosis, but no endocytosis was observed when the cells were transfected with LMO7b-S727A,S1295A (Fig. 5A). When we further analyzed the effect of individually mutated Ser-727 and Ser-1295, we found that only the replacement of Ser-1295 prevented the high CO_2-induced Na,K-ATPase endocytosis (Fig. 5A). Moreover, FLAG-LMO7b-S1295A is less phosphorylated in the *in vitro* kinase assay (Fig. 5B, left), while FLAG-LMO7b-S727A, FLAG-LMO7b-S1300A, and FLAG-LMO7b-S1305A are phosphorylated to approximately the same extent as FLAG-LMO7b-WT (Fig. 5B, middle), suggesting that the phosphorylation of LMO7b at Ser-1295 is required for Na,K-ATPase endocytosis during hypercapnia.

JNK-induced phosphorylation of LMO7b is required for its interaction with Na,K-ATPase during hypercapnia. Microscopy analysis of endogenous LMO7b shows a plasma membrane and cytoplasmic distribution (Fig. 6A). In untreated rATII cells, LMO7b (red) localized mostly at the apical side and Na,K-ATPase (green) at the lateral side of the cells, and minimal colocalization was observed, as demonstrated in the vertical sections of the cell generated from confocal z-stack images (Fig. 6A). In the presence of high CO_2, there was a redistribution of LMO7b from the apical to the lateral domains, where its colocalization with Na,K-ATPase was increased (Fig. 6A [arrows], B, [CO_2], and C) compared to the control cells (Fig. 6A [arrowheads], B, [CT], and C). Figure 6B shows that exposure to high CO_2 increases the plasma membrane colocalization between Na,K-ATPase and LMO7b. Importantly, the inhibition of JNK prevented a hypercapnia-induced increase in colocalization between Na,K-ATPase and LMO7b. Taken together, these results suggest that high CO_2 induces JNK-dependent LMO7b phosphorylation, which triggers the redistribution of LMO7b to the lateral membrane, where it colocalizes and presumably interacts with Na,K-ATPase.

We confirmed the interaction between Na,K-ATPase and LMO7b during hypercapnia in A549-GFP-α_1 cells transiently transfected with rat FLAG-LMO7b. Immunoprecipitation with a GFP antibody showed increased coimmunoprecipitation of

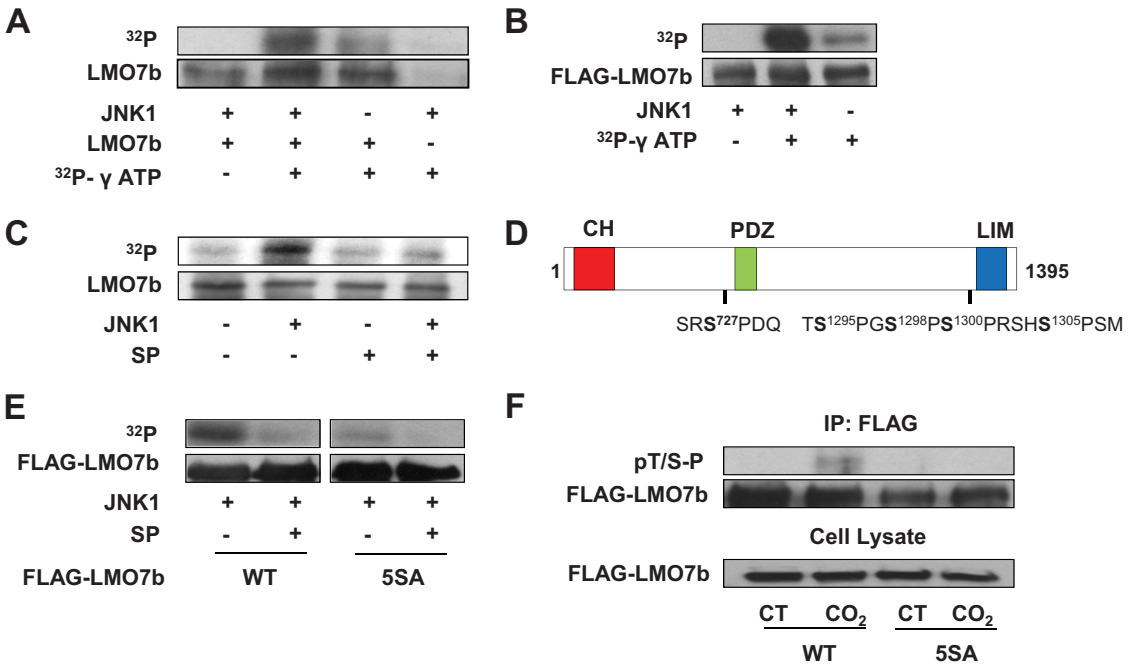

FIG 3 LMO7b is a target for JNK phosphorylation. (A) *In vitro* JNK kinase assay was performed by incubating purified recombinant JNK1 (150 ng) with LMO7b immunoprecipitated (IP) from rATII cells in the presence or absence of [γ-^{32}P]ATP. A representative autoradiograph of phosphorylated LMO7b (^{32}P) and Western blot (WB) of LMO7b are shown. $n = 3$. (B) *In vitro* JNK kinase assay using rat FLAG-LMO7b as a substrate immunoprecipitated from A549 transfected cells. $n = 3$. (C) *In vitro* kinase assay was performed in the presence or absence of SP600125 (20 μM) as described for panel A. A representative autoradiograph of phosphorylated LMO7b (^{32}P) and WB analysis of LMO7b are shown. $n = 3$. (D) A schematic depicting rat LMO7b potential JNK phosphorylation sites. (E) *In vitro* JNK kinase assay was performed as described for panel A using LMO7b-FLAG (WT) or FLAG-LMO7b bearing a serine-to-alanine mutation in positions 727, 1295, 1298, 1300, and 1305 (FLAG-LMO7b-5SA). A representative autoradiograph of phosphorylated LMO7 (^{32}P) and WB analysis of LMO7 using FLAG antibody are shown. $n = 3$. (F) A549 cells were transfected with FLAG-LMO7b-WT or FLAG-LMO7b-5SA, and 48 h later cells were exposed for 10 min to either normocapnia (CT) or hypercapnia (CO_2). LMO7b was immunoprecipitated using FLAG antibody, and the phosphorylation of LMO7 was analyzed by WB using a pT/S-P antibody. The total amount of immunoprecipitated LMO7b was measured using FLAG antibody. $n = 3$.

LMO7b in hypercapnia compared to that of the control (Fig. 7A). The interaction between Na,K-ATPase and LMO7b was prevented in cells pretreated with SP600125 and, importantly, in cells transfected with LMO7b-S1295A (Fig. 7), supporting the functional role of LMO7b phosphorylation and in agreement with the immunofluorescence data.

Hypercapnia increases the interaction of LMO7b with proteins of the endocytic pathway. It has been described that in epithelial lung and kidney cells, Na,K-ATPase endocytosis during hypoxia or dopamine stimulation is clathrin dependent (30, 38). Interestingly, we observed that hypercapnia increases the interaction of Na,K-ATPase with the clathrin heavy chain (Fig. 8A).

To explore the mechanism by which LMO7b plays a role in Na,K-ATPase endocytosis during hypercapnia, we assessed the proteins coimmunoprecipitated with LMO7b in rATII cells exposed to high CO_2. Besides the Na,K-ATPase α subunit, the analysis identified several proteins whose interactions with LMO7b were increased during hypercapnia (Fig. 8B, LMO7b bound CO_2/CT) without changing their total levels. The list of proteins whose binding to LMO7b increased during hypercapnia includes proteins that are required for clathrin-dependent endocytosis and vesicular trafficking. In particular, the interaction between LMO7b and adaptor binding protein complex 2-beta subunit (AP2-β) is increased by hypercapnia. AP2-β mediates the formation of endocytic clathrin-coated vesicles from the plasma membrane by binding to clathrin (39–41). Other hypercapnia-induced LMO7b-interacting proteins include proteins that are involved in vesicular trafficking and/or membrane fusion, like cytoplasmic dynein 1 heavy chain 1 (42), Rab GTPase-binding effector protein 1 (43), cofilin 1 (44–46), septins (47, 48), and Huntingtin-interacting protein 1 related (Hip1R) (49). Ezrin is involved in, among other functions, cytoskeletal anchoring at the plasma membrane (50). Protein phosphatase 1 regulatory subunit 12 was another protein that was identified which has been described to bind 14-3-3 protein and act as a signal transductor during endocytosis (51). As such, our results suggest that the phosphorylation of LMO7b downstream JNK activation during hypercapnia promotes the interaction and/or binding with multiple members of the clathrin-dependent endocytic pathway as well as with Na,K-ATPase, facilitating the endocytic process.

DISCUSSION

Hypercapnia impairs alveolar epithelial function by promoting Na,K-ATPase endocytosis *in vivo* and *in vitro* via the phosphorylation and activation of JNK downstream of AMPK and PKCζ (5–7). Here, we show that during hypercapnia, JNK activation promotes the phosphorylation of LMO7b, followed by its colocalization and interaction with the Na,K-ATPase and several components of the clathrin-dependent endocytic machinery. *In vitro* kinase assays and studies in cultured cells suggest that JNK phosphorylates LMO7b at Ser-1295. Moreover, LMO7b silencing or overexpression of LMO7b-S1295A inhibited high CO_2-in-

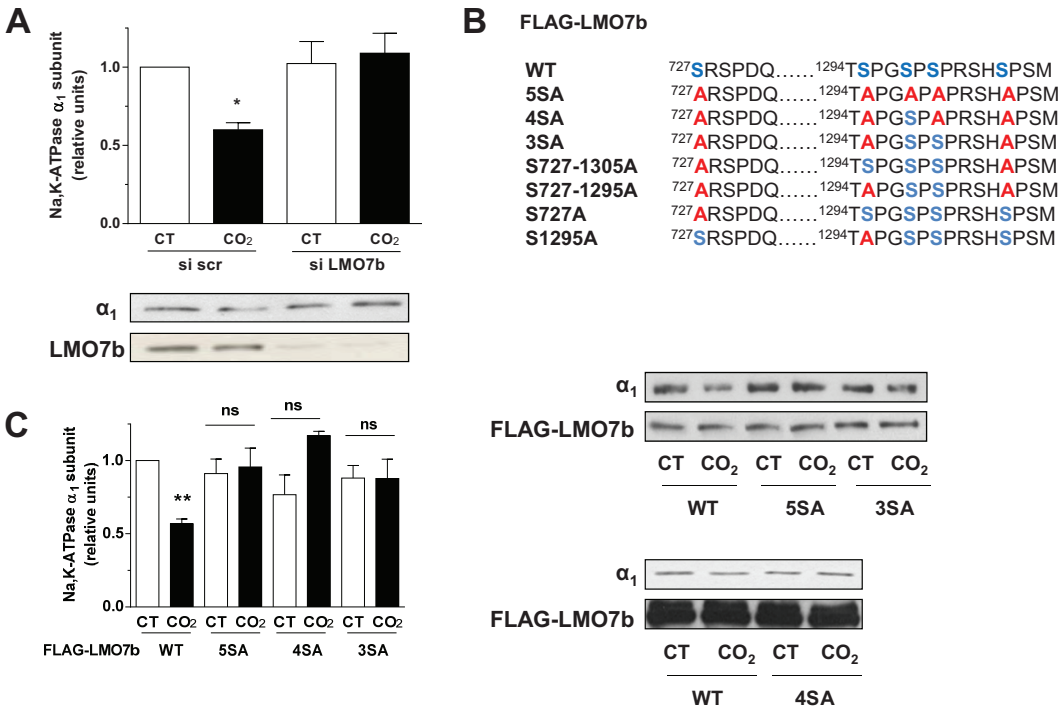

FIG 4 Hypercapnia-induced Na,K-ATPase endocytosis requires LMO7b phosphorylation. (A) A549 cells were transfected with an siRNA against LMO7b (si LMO7b) or scrambled siRNA (si scr) and exposed for 30 min to either normocapnia (CT) or hypercapnia (CO_2). Na,K-ATPase at the plasma membrane was determined by biotin-streptavidin pulldown and Western blotting (WB). Representative WB of Na,K-ATPase-α_1 and LMO7 are shown. Values are expressed as means ± SEM. $n = 3$. (B) Schematic depicting the different FLAG-LMO7b constructs used. (C) A549 cells were transfected with FLAG-LMO7b-WT, FLAG-LMO7b-5SA, FLAG-LMO7b-4SA, and FLAG-LMO7b-3SA, and 48 h later cells were exposed for 10 min to either normocapnia or hypercapnia. Na,K-ATPase expression at the plasma membrane was performed as described for panel A. Values are expressed as means ± SEM. $n = 3$. *, $P < 0.05$; **, $P < 0.01$.

duced Na,K-ATPase endocytosis. These findings contribute to our understanding of the regulation of Na,K-ATPase expression at the plasma membrane of epithelial cells during hypercapnia and to the regulation of Na^+ transport, which is essential for the optimal function of the alveolar epithelium.

We have reported that Na,K-ATPase endocytosis during hypercapnia requires the activation of JNK; however, JNK does not phosphorylate the Na,K-ATPase (6). Our current study suggested that LMO7b is a substrate for JNK in alveolar epithelial cells exposed to elevated CO_2. LMO7, an actin-binding protein widely expressed in adult tissues and particularly in lung epithelial cells (27, 28), belongs to a family of nine proteins that contain both PDZ and LIM domains. These domains function as protein-protein recognition modules and play a role in the maintenance of epithelial cell architecture (28). The expression of LMO7 is cell type specific, and in agreement with previous publications (52), we found that rat alveolar type II cells express only LMO7b. These results agree with previous reports that LMO7a (220 kDa) is expressed only in embryonic stem cells (28). It has been described that in normal bronchial epithelium LMO7 usually is localized to the apical membranes, while normal alveolar cells display circumferential staining of the entire cell membrane (52). MAPKs usually phosphorylate a serine or threonine followed by a proline, and LMO7b has five such sequences (Fig. 4B). We determined that high CO_2 exposure results in the phosphorylation of LMO7b in a time- and concentration-dependent manner. Furthermore, this phosphorylation was prevented by pharmacologically or genetically inhibiting JNK or by overexpressing a dominant-negative form of AMPK, which acts upstream of JNK. An *in vitro* kinase assay suggested that JNK induces LMO7b phosphorylation and that when the five serines in the Ser-Pro domains (Ser-727, Ser-1295, Ser-1298, Ser-1300, and Ser-1305) were mutated to alanine, the phosphorylation was prevented. In the absence of JNK, a low level of phosphorylation still was observed; this could be the result of LMO7b phosphorylation by another kinase that coprecipitates with LMO7b and that is not inhibited by SP600125, suggesting that LMO7b also is the substrate of other kinases. Importantly, FLAG-LMO7b-5SA failed to be phosphorylated *in vivo* in response to CO_2 (Fig. 3F). Interestingly, LMO7b exhibits the amino acid sequence ^{1030}**K**LQER**L**M**L**^{1037}, which follows the JNK binding domain (JBD) consensus sequence, which generally has the pattern R/K_{2-3}-X_{1-6}-L/I-X-L/I, similar to the one present in c-jun (^{33}I-L-K-Q-S-M-T-L-N-L-A^{43}), a bona fide JNK substrate, and it is considered a JNK binding domain (53). The presence of a JBD usually enhances the efficiency and specificity of phosphorylation and/or mediates the interaction with upstream activators, substrates, or scaffolding molecules (19, 54).

The inhibition of JNK prevents Na,K-ATPase endocytosis during hypercapnia (6), and silencing of LMO7b or overexpressing FLAG-LMO7b-5SA in alveolar epithelial cells inhibited the hypercapnia-induced Na,K-ATPase endocytosis, suggesting a physiological role for the phosphorylation of LMO7b during hypercapnia. Moreover, using an *in vitro* kinase assay and cell surface biotinylation and coimmunoprecipitation experiments, we identified Ser-1295 as a new phosphorylation site which is required for high CO_2-dependent Na,K-ATPase endocytosis. Due to the pres-

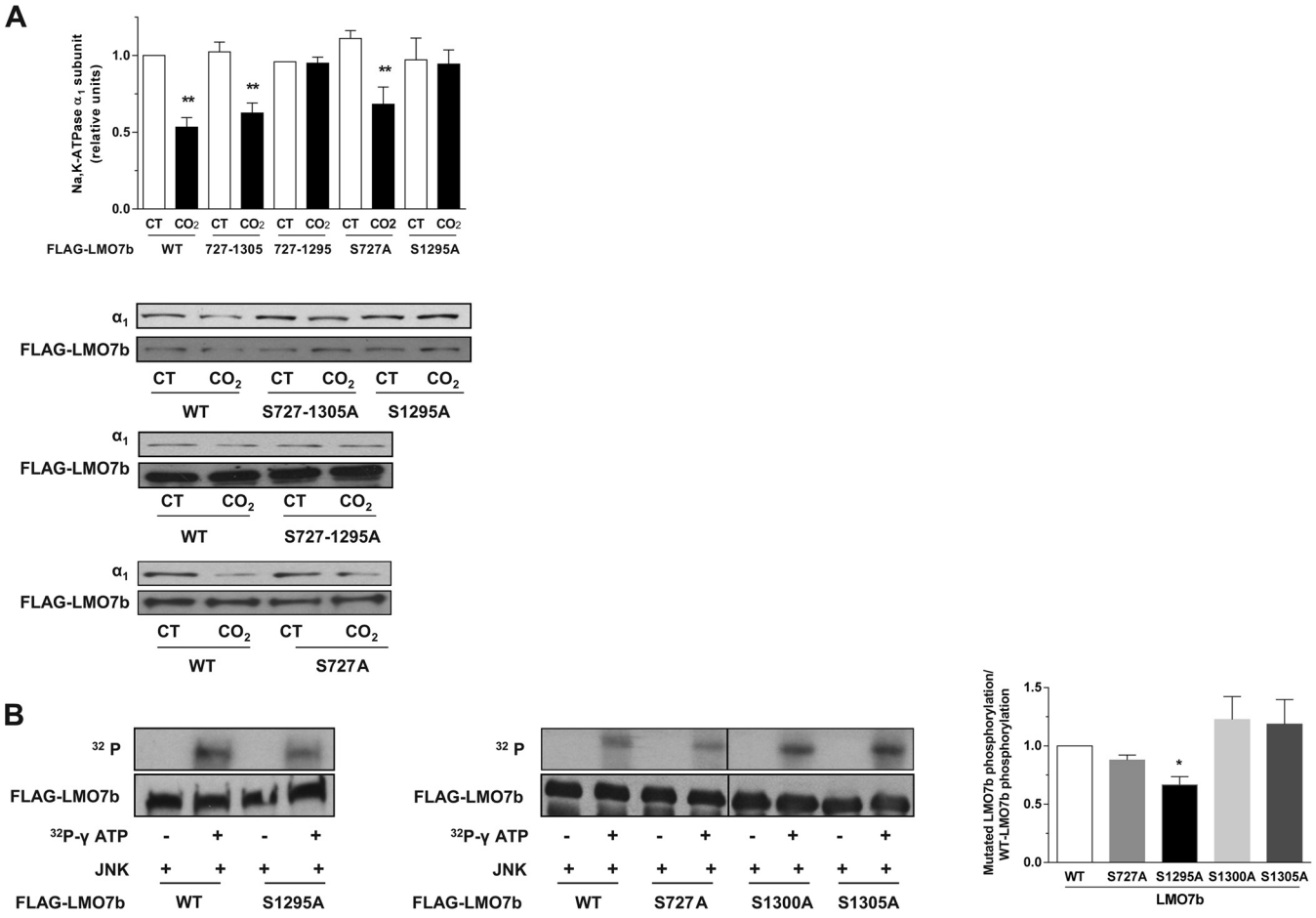

FIG 5 LMO7b is phosphorylated at Ser-1295 during hypercapnia. (A) A549 cells were transfected at FLAG-LMO7b-WT, FLAG-LMO7b-S727A-S1305A, FLAG-LMO7b-S727A-S1295A, FLAG-LMO7b-S727A, or FLAG-LMO7b-S1295A, and 48 h later cells were exposed for 30 min to either normocapnia (CT) or hypercapnia (CO_2). Na,K-ATPase expression at the plasma membrane was determined by biotin-streptavidin pulldown and Western blotting (WB). Representative WB of Na,K-ATPase-α_1 and FLAG are shown. Values are expressed as means ± SEM. $n = 3$. (B) *In vitro* JNK kinase assay was performed by incubating purified recombinant JNK1 (150 ng) with FLAG-LMO7b-WT, FLAG-LMO7b-S727A, FLAG-LMO7b-S1295A, FLAG-LMO7b-S1300A, and FLAG-LMO7b-S1305A immunoprecipitated from A549 cells in the presence or absence of [γ-^{32}P]ATP. A representative autoradiography of phosphorylated LMO7b (^{32}P) and WB of FLAG-LMO7b are shown. (Right) Quantification of the phosphorylation levels in the different immunoprecipitated mutants. Values shown are means ± SEM. $n = 3$. *, $P < 0.05$; **, $P < 0.01$.

ence of the protein-protein interaction PDZ and LIM domains, LMO7b may act as a scaffold, binding to filamentous actin-associated proteins (27, 28). Ser-1295 is adjacent to the LIM domain (amino acids 1326 to 1384) and is part of the C-terminal proline-rich domain (TSPGSPSPR). Interestingly, it has been described that JNK phosphorylates a very similar proline-rich domain (TPGTPGTPS) located in the C terminus of microtubule-associated protein 2 in dendritic cells (55). One possible mechanism is that Ser-1295 phosphorylation in response to high CO_2 alters the conformational profile of the adjacent LIM domain and/or other regions of the molecule, promoting the formation of a complex containing Na,K-ATPase, JNK, and possibly other molecules. This hypothesis is supported by the fact that, in the untreated/unphosphorylated state, LMO7b is located mostly at the apical membrane of the alveolar epithelial cells, where it does not interact with Na,K-ATPase, while the phosphorylation of Ser-1295 results in a relocalization to the lateral membrane (Fig. 6A). JNK-mediated phosphorylation may change the activity of its substrates; however, in some cases, it has been described that the phosphorylation-dependent changes are more complex and involve changes in protein binding and/or localization in the cell (19). Our coimmunoprecipitation studies demonstrate a physical interaction between Na,K-ATPase and LMO7b even under normocapnic conditions, which is increased after exposure to hypercapnia. This interaction is dependent both on JNK activity and on the phosphorylation of LMO7b at Ser-1295 (Fig. 6 and 7). Taken together, these data demonstrate that the physical interaction of LMO7b and Na,K-ATPase under hypercapnic conditions is dependent on LMO7b Ser-1295 phosphorylation by JNK.

We have previously described that in response to a variety of signals, Na,K-ATPase endocytosis occurs via a clathrin-dependent mechanism and interacts with AP2 (30, 38, 56). In agreement with these results, the exposure of the cells to hypercapnia results in the increased interaction of the Na,K-ATPase-α_1 subunit not only with FLAG-LMO7b but also with clathrin heavy chain (Fig. 8A), suggesting that LMO7b contributes to the formation of the endocytic vesicles. Interestingly, the mass spec-

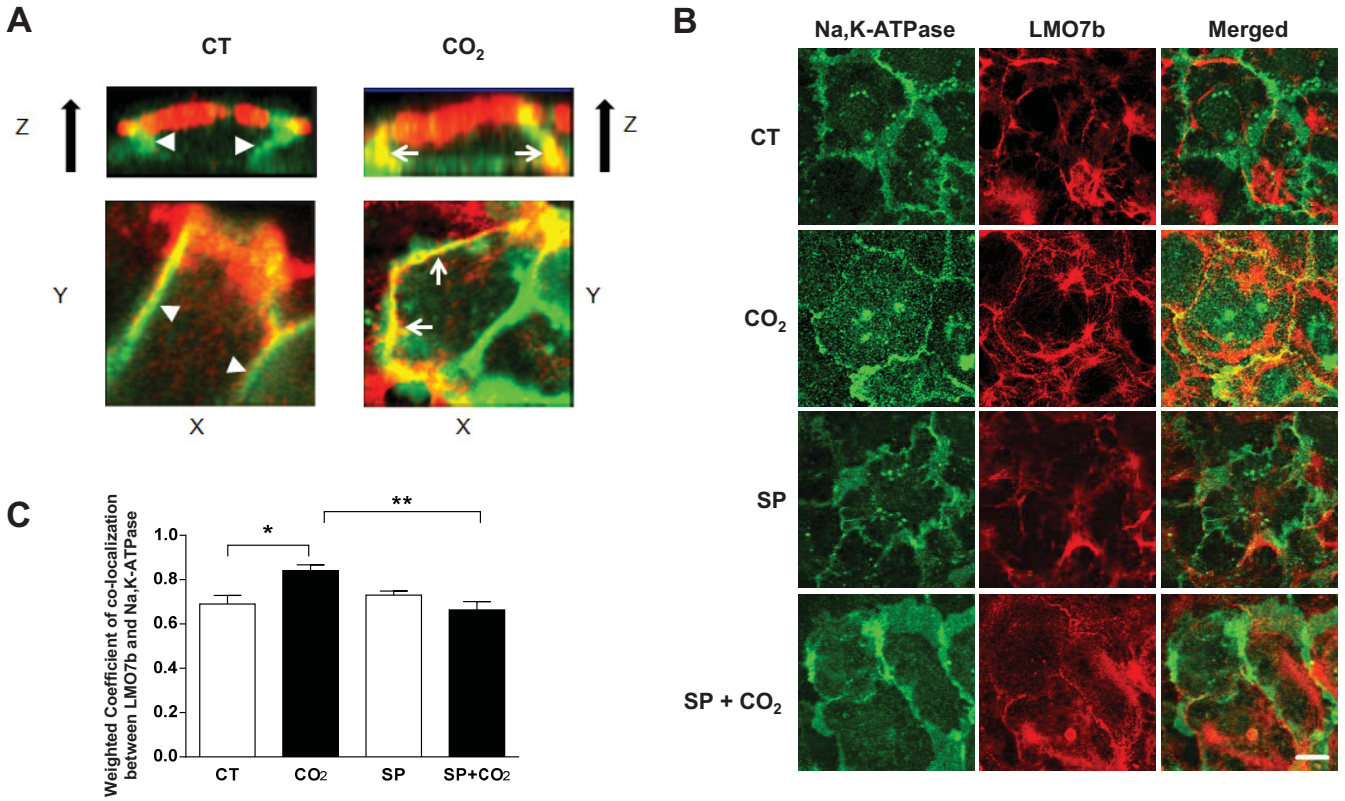

FIG 6 LMO7b colocalizes with Na,K-ATPase during hypercapnia. (A) Immunofluorescence images of rATII cells exposed for 15 min to either normocapnia (CT) or hypercapnia (CO_2). The merged images were assessed by indirect multichannel acquisition. The green channel represents Na,K-ATPase-α_1, the red channel represents LMO7b, and yellow indicates colocalization. z-stacks were collected at stepwise z increments from the basal to the apical side of the cell. (B) Immunofluorescence images of rATII cells exposed for 15 min to either normocapnia or hypercapnia in the presence or absence of SP600125 (SP; 20 μM for 30 min). The merged images were assessed by indirect multichannel acquisition. The green channel represents Na,K-ATPase-α_1, the red channel represents LMO7b, and yellow indicates colocalization. (C) Quantification of the colocalization of Na,K-ATPase-α_1 and LMO7b. At least 7 images where analyzed for each condition. *, $P < 0.05$; **, $P < 0.01$.

troscopy analysis of LMO7b interacting partners identified several proteins that play a role in clathrin-mediated endocytosis. One of the proteins whose interaction with LMO7b is increased during hypercapnia is the AP2-β subunit, which links clathrin to the cargo protein (39, 40). Other proteins identified play different roles during endocytosis. Collectively, our results suggest that LMO7b phosphorylation serves as a signal to promote the organization of the forming vesicle or for the recruitment of proteins to the vesicle. LMO7b is a multidomain protein which binds to actin and also possesses LIM and PDZ domains, which are involved in interactions with other proteins (27). LMO7b may act as a scaffolding protein by bringing together the actin cytoskeleton with the endocytic machinery and Na,K-ATPase, facilitating the endocytic flow.

In summary, we provide evidence that LMO7b is important in hypercapnia-induced Na,K-ATPase endocytosis. JNK-induced

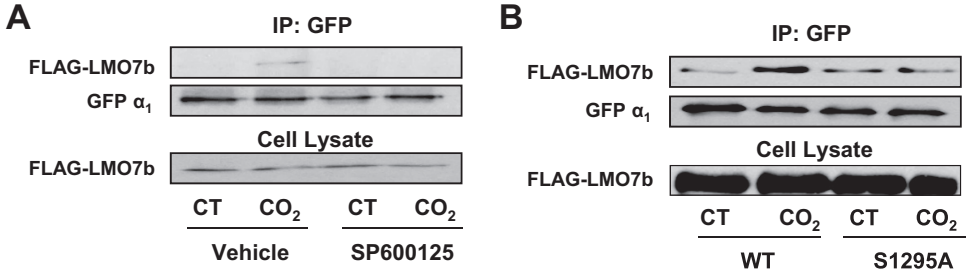

FIG 7 JNK-induced phosphorylation of LMO7b at Ser-1295 is required for Na,K-ATPase-LMO7b interaction during hypercapnia. (A) A549-GFP-α_1 cells were transfected with LMO7b-FLAG-WT, and 48 h later cells were exposed for 15 min to either normocapnia (CT) or hypercapnia (CO_2) in the presence of SP600125 (20 μM; 30-min preincubation) or dimethyl sulfoxide (DMSO) (vehicle). Cells were lysed using a low-detergent buffer, and Na,K-ATPase-α_1 subunit was immunoprecipitated (IP) using GFP antibody. Representative WB showing Na,K-ATPase-α_1 subunit or LMO7b are shown. $n = 3$. (B) A549-GFP-α_1 cells were transfected with FLAG-LMO7b-WT or FLAG-LMO7b-S1295A, and 48 h later cells were exposed for 15 min to either normocapnia or hypercapnia and processed as described for panel A. $n = 3$.

A

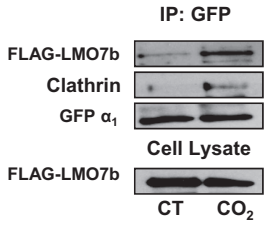

B

Accession	Description	Coverage	# Unique Peptides	# Peptides	LMO7b-bound CO_2/CT normalized by LMO7b	LMO7b-bound CO_2/CT Variability [%]	Total CO_2/CT normalized by LMO7b	Total CO_2/CT Variability [%]
Q6AYQ4	Transmembrane protein 109	11.52%	1	2	2.59	0.7	0.67	33.5
P62944	**AP-2 complex subunit beta**	8.11%	2	7	1.94	2.8	0.95	20.1
A0JPM9	Eukaryotic translation initiation factor 3 subunit J	30.12%	3	8	1.92	9.9	0.81	
D3ZH41	**Cytoskeleton-associated protein 4**	10.43%	1	3	1.83	6.5	0.73	16
P62870	Transcription elongation factor B polypeptide 2	35.59%	5	6	1.79	21.8	0.65	21.7
F1LRT9	Cytoplasmic dynein 1 heavy chain 1	12.47%	5	53	1.73	17.4	0.90	21.8
Q68FR9-2	Isoform 2 of Elongation factor 1-delta	19.54%	5	13	1.64	7.9	0.81	5.5
D3ZIC4	**Protein phosphatase 1 regulatory subunit 12**	11.98%	1	13	1.61		0.48	
P83941	Transcription elongation factor B polypeptide 1	31.25%	3	3	1.55	0.1	0.72	
P62986	Ubiquitin-60S ribosomal protein L40	46.09%	2	7	1.53	11.7	0.95	16.9
B5DEN5	Eukaryotic translation elongation factor 1 beta	22.22%	3	5	1.52	4.8	0.86	11.9
Q9R0T4	Cadherin-1	4.18%	1	4	1.49		0.90	6.9
P63074	**Eukaryotic translation initiation factor 4E**	17.05%	1	4	1.45		0.62	28.3
P04692-3	Isoform 3 of Tropomyosin alpha-1 chain	35.94%	1	14	1.42	8	0.84	14.4
P41542	General vesicular transport factor p115	8.03%	1	7	1.40		0.98	11.7
G3V9J7	Rab GTPase-binding effector protein 1	14.73%	3	12	1.39	22.6	none	
P45592	**Cofilin-1**	18.67%	2	3	1.36	7.6	0.92	12.7
Q63610	Tropomyosin alpha-3 chain	54.03%	3	16	1.35	5.5	0.83	15.8
F1LML7	**Protein Hip1r**	27.78%	15	32	1.34	14.9	no quant	
Q07936	Annexin A2	36.28%	4	11	1.34	20.8	1.13	10.8
P62628	Dynein light chain roadblock-type 1	12.50%	1	1	1.31		0.80	5
Q64119	Myosin light polypeptide 6	41.06%	5	6	1.31	13.7	0.83	11
P31977	**Ezrin**	17.41%	2	10	1.24	18	0.85	6.4
Q91Y81	**Septin-2**	11.36%	1	5	1.17		0.77	6.1
G3V6P7	Myosin, heavy polypeptide 9, non-muscle	35.87%	31	72	1.16	14.3	0.87	14.1

FIG 8 Hypercapnia increases the interaction of LMO7b with endocytic proteins. (A) A549-GFP-α_1 cells were transfected with LMO7b-FLAG-WT, and 48 h later cells were exposed for 15 min to either normocapnia (CT) or hypercapnia (CO_2). Cells were lysed using a low-detergent buffer, and Na,K-ATPase-α_1 subunit was immunoprecipitated (IP) using GFP antibody. Representative WB showing Na,K-ATPase-α_1 subunit or LMO7b are shown. $n = 3$. (B) rATII cells were exposed to normocapnia or hypercapnia for 15 min. Cells were lysed as described for panel A, and LMO7b was immunoprecipitated with the LMO7b M300 antibody and processed as described in Materials and Methods. The table depicts proteins that coimmunoprecipitated with LMO7b as analyzed by nLC MS/MS. Endocytosis-related proteins are shown in boldface. $n = 3$.

phosphorylation of LMO7b at Ser-1295 regulates the interaction between LMO7b and Na,K-ATPase, promoting Na,K-ATPase endocytosis. We hypothesize that LMO7b plays a scaffolding role, bringing together Na,K-ATPase and molecules required for its endocytosis.

ACKNOWLEDGMENTS

This work was supported in part by HL-48129 and HL-85534 (to L.A.D., Y.G., and J.I.S.).

The Universities of Giessen and Marburg Lung Center is a member of the German Center for Lung Research.

We have no conflicts of interest to declare.

REFERENCES

1. **Kessler R, Faller M, Fourgaut G, Mennecier B, Weitzenblum E.** 1999. Predictive factors of hospitalization for acute exacerbation in a series of 64 patients with chronic obstructive pulmonary disease. Am J Respir Crit Care Med **159:**158–164. http://dx.doi.org/10.1164/ajrccm.159.1.9803117.
2. **Vitacca M, Bianchi L, Barbano L, Ziliani M, Ambrosino N.** 2005. Effects of acute on chronic respiratory failure on hypercapnia and 3-month survival. Chest **128:**1209–1215. http://dx.doi.org/10.1378/chest.128.3.1209.
3. **Vadasz I, Hubmayr RD, Nin N, Sporn PH, Sznajder JI.** 2012. Hypercapnia: a nonpermissive environment for the lung. Am J Respir Cell Mol Biol **46:**417–421. http://dx.doi.org/10.1165/rcmb.2011-0395PS.
4. **Kohnlein T, Windisch W, Wegscheider K, Welte T.** 2014. Non-invasive positive pressure ventilation for severe COPD. Authors' reply. Lancet Respir Med **2:**e19.
5. **Briva A, Vadasz I, Lecuona E, Welch LC, Chen J, Dada LA, Trejo HE, Dumasius V, Azzam ZS, Myrianthefs PM, Batlle D, Gruenbaum Y, Sznajder JI.** 2007. High CO2 levels impair alveolar epithelial function independently of pH. PLoS One **2:**e1238. http://dx.doi.org/10.1371/journal.pone.0001238.
6. **Vadasz I, Dada LA, Briva A, Helenius IT, Sharabi K, Welch LC, Kelly AM, Grzesik BA, Budinger GR, Liu J, Seeger W, Beitel GJ, Gruenbaum Y, Sznajder JI.** 2012. Evolutionary conserved role of c-Jun-N-terminal kinase in CO2-induced epithelial dysfunction. PLoS One **7:**e46696. http://dx.doi.org/10.1371/journal.pone.0046696.
7. **Vadasz I, Dada LA, Briva A, Trejo HE, Welch LC, Chen J, Toth PT, Lecuona E, Witters LA, Schumacker PT, Chandel NS, Seeger W, Sznajder JI.** 2008. AMP-activated protein kinase regulates CO2-induced alveolar epithelial dysfunction in rats and human cells by promoting Na,K-ATPase endocytosis. J Clin Investig **118:**752–762.
8. **Sznajder JI.** 2001. Alveolar edema must be cleared for the acute respiratory distress syndrome patient to survive. Am J Respir Crit Care Med **163:**1293–1294. http://dx.doi.org/10.1164/ajrccm.163.6.ed1801d.
9. **Berthiaume Y, Folkesson HG, Matthay MA.** 2002. Lung edema clearance: 20 years of progress: invited review: alveolar edema fluid clearance in the injured lung. J Appl Physiol **93:**2207–2213. http://dx.doi.org/10.1152/japplphysiol.01201.2001.
10. **Dada LA, Chandel NS, Ridge KM, Pedemonte C, Bertorello AM, Sznajder JI.** 2003. Hypoxia-induced endocytosis of Na,K-ATPase in alveolar epithelial cells is mediated by mitochondrial reactive oxygen species and PKC-zeta. J Clin Investig **111:**1057–1064. http://dx.doi.org/10.1172/JCI16826.
11. **Mutlu GM, Sznajder JI.** 2005. Mechanisms of pulmonary edema clearance. Am J Physiol Lung Cell Mol Physiol **289:**L685–L695. http://dx.doi.org/10.1152/ajplung.00247.2005.
12. **Factor P, Senne C, Dumasius V, Ridge K, Jaffe HA, Uhal B, Gao Z, Sznajder JI.** 1998. Overexpression of the Na+,K+-ATPase alpha1 subunit increases Na+,K+-ATPase function in A549 cells. Am J Respir Cell Mol Biol **18:**741–749. http://dx.doi.org/10.1165/ajrcmb.18.6.2918.
13. **Shull GE, Schwartz A, Lingrel JB.** 1985. Amino-acid sequence of the catalytic subunit of the (Na+ + K+)ATPase deduced from a complementary DNA. Nature **316:**691–695. http://dx.doi.org/10.1038/316691a0.
14. **Looney MR, Sartori C, Chakraborty S, James PF, Lingrel JB, Matthay MA.** 2005. Decreased expression of both the alpha1- and alpha2-subunits

of the Na-K-ATPase reduces maximal alveolar epithelial fluid clearance. Am J Physiol Lung Cell Mol Physiol **289:**L104–L110. http://dx.doi.org/10.1152/ajplung.00464.2004.
15. **Sznajder JI, Factor P, Ingbar DH.** 2002. Invited review: lung edema clearance: role of Na(+)-K(+)-ATPase. J Appl Physiol **93:**1860–1866. http://dx.doi.org/10.1152/japplphysiol.00022.2002.
16. **Gusarova GA, Dada LA, Kelly AM, Brodie C, Witters LA, Chandel NS, Sznajder JI.** 2009. Alpha1-AMP-activated protein kinase regulates hypoxia-induced Na,K-ATPase endocytosis via direct phosphorylation of protein kinase C zeta. Mol Cell Biol **29:**3455–3464. http://dx.doi.org/10.1128/MCB.00054-09.
17. **Lecuona E, Sun H, Chen J, Trejo HE, Baker MA, Sznajder JI.** 2013. Protein kinase A-Ialpha regulates Na,K-ATPase endocytosis in alveolar epithelial cells exposed to high CO(2) concentrations. Am J Respir Cell Mol Biol **48:**626–634. http://dx.doi.org/10.1165/rcmb.2012-0373OC.
18. **Raman M, Chen W, Cobb MH.** 2007. Differential regulation and properties of MAPKs. Oncogene **26:**3100–3112. http://dx.doi.org/10.1038/sj.onc.1210392.
19. **Bogoyevitch MA, Kobe B.** 2006. Uses for JNK: the many and varied substrates of the c-Jun N-terminal kinases. Microbiol Mol Biol Rev **70:**1061–1095. http://dx.doi.org/10.1128/MMBR.00025-06.
20. **Huang C, Rajfur Z, Borchers C, Schaller MD, Jacobson K.** 2003. JNK phosphorylates paxillin and regulates cell migration. Nature **424:**219–223. http://dx.doi.org/10.1038/nature01745.
21. **Mengistu M, Brotzman H, Ghadiali S, Lowe-Krentz L.** 2011. Fluid shear stress-induced JNK activity leads to actin remodeling for cell alignment. J Cell Physiol **226:**110–121. http://dx.doi.org/10.1002/jcp.22311.
22. **Chen Z, Gibson TB, Robinson F, Silvestro L, Pearson G, Xu B, Wright A, Vanderbilt C, Cobb MH.** 2001. MAP kinases. Chem Rev **101:**2449–2476. http://dx.doi.org/10.1021/cr000241p.
23. **Lee MH, Koria P, Qu J, Andreadis ST.** 2009. JNK phosphorylates beta-catenin and regulates adherens junctions. FASEB J **23:**3874–3883. http://dx.doi.org/10.1096/fj.08-117804.
24. **Lee MH, Padmashali R, Koria P, Andreadis ST.** 2011. JNK regulates binding of alpha-catenin to adherens junctions and cell-cell adhesion. FASEB J **25:**613–623. http://dx.doi.org/10.1096/fj.10-161380.
25. **Pearson G, Robinson F, Beers Gibson T, Xu BE, Karandikar M, Berman K, Cobb MH.** 2001. Mitogen-activated protein (MAP) kinase pathways: regulation and physiological functions. Endocr Rev **22:**153–183.
26. **Katz S, Aronheim A.** 2002. Differential targeting of the stress mitogen-activated protein kinases to the c-Jun dimerization protein 2. Biochem J **368:**939–945. http://dx.doi.org/10.1042/bj20021127.
27. **Ooshio T, Irie K, Morimoto K, Fukuhara A, Imai T, Takai Y.** 2004. Involvement of LMO7 in the association of two cell-cell adhesion molecules, nectin and E-cadherin, through afadin and alpha-actinin in epithelial cells. J Biol Chem **279:**31365–31373. http://dx.doi.org/10.1074/jbc.M401957200.
28. **Tanaka-Okamoto M, Hori K, Ishizaki H, Hosoi A, Itoh Y, Wei M, Wanibuchi H, Mizoguchi A, Nakamura H, Miyoshi J.** 2009. Increased susceptibility to spontaneous lung cancer in mice lacking LIM-domain only 7. Cancer Sci **100:**608–616. http://dx.doi.org/10.1111/j.1349-7006.2009.01091.x.
29. **Ridge KM, Olivera WG, Saldias F, Azzam Z, Horowitz S, Rutschman DH, Dumasius V, Factor P, Sznajder JI.** 2003. Alveolar type 1 cells express the alpha2 Na,K-ATPase, which contributes to lung liquid clearance. Circ Res **92:**453–460. http://dx.doi.org/10.1161/01.RES.0000059414.10360.F2.
30. **Chen Z, Krmar RT, Dada L, Efendiev R, Leibiger IB, Pedemonte CH, Katz AI, Sznajder JI, Bertorello AM.** 2006. Phosphorylation of adaptor protein-2 mu2 is essential for Na+,K+-ATPase endocytosis in response to either G protein-coupled receptor or reactive oxygen species. Am J Respir Cell Mol Biol **35:**127–132. http://dx.doi.org/10.1165/rcmb.2006-0044OC.
31. **Bradford MM.** 1976. A rapid and sensitive method for the quantitation of microgram quantities of protein utilizing the principle of protein-dye binding. Anal Biochem **72:**248–254. http://dx.doi.org/10.1016/0003-2697(76)90527-3.
32. **Hallows KR, Kobinger GP, Wilson JM, Witters LA, Foskett JK.** 2003. Physiological modulation of CFTR activity by AMP-activated protein kinase in polarized T84 cells. Am J Physiol Cell Physiol **284:**C1297–C1308. http://dx.doi.org/10.1152/ajpcell.00227.2002.
33. **Vagin O, Tokhtaeva E, Garay PE, Souda P, Bassilian S, Whitelegge JP, Lewis R, Sachs G, Wheeler L, Aoki R, Fernandez-Salas E.** 2014. Recruitment of septin cytoskeletal proteins by botulinum toxin A protease determines its remarkable stability. J Cell Sci **127:**3294–3308. http://dx.doi.org/10.1242/jcs.146324.
34. **Boersema PJ, Raijmakers R, Lemeer S, Mohammed S, Heck AJ.** 2009. Multiplex peptide stable isotope dimethyl labeling for quantitative proteomics. Nat Protoc **4:**484–494. http://dx.doi.org/10.1038/nprot.2009.21.
35. **Rappsilber J, Mann M, Ishihama Y.** 2007. Protocol for micro-purification, enrichment, pre-fractionation and storage of peptides for proteomics using StageTips. Nat Protoc **2:**1896–1906. http://dx.doi.org/10.1038/nprot.2007.261.
36. **Al-Khalili L, Kotova O, Tsuchida H, Ehren I, Feraille E, Krook A, Chibalin AV.** 2004. ERK1/2 mediates insulin stimulation of Na(+),K(+)-ATPase by phosphorylation of the alpha-subunit in human skeletal muscle cells. J Biol Chem **279:**25211–25218. http://dx.doi.org/10.1074/jbc.M402152200.
37. **Khundmiri SJ, Bertorello AM, Delamere NA, Lederer ED.** 2004. Clathrin-mediated endocytosis of Na+,K+-ATPase in response to parathyroid hormone requires ERK-dependent phosphorylation of Ser-11 within the alpha1-subunit. J Biol Chem **279:**17418–17427. http://dx.doi.org/10.1074/jbc.M311715200.
38. **Chibalin AV, Ogimoto G, Pedemonte CH, Pressley TA, Katz AI, Feraille E, Berggren PO, Bertorello AM.** 1999. Dopamine-induced endocytosis of Na+,K+-ATPase is initiated by phosphorylation of Ser-18 in the rat alpha subunit and is responsible for the decreased activity in epithelial cells. J Biol Chem **274:**1920–1927. http://dx.doi.org/10.1074/jbc.274.4.1920.
39. **Ohno H.** 2006. Clathrin-associated adaptor protein complexes. J Cell Sci **119:**3719–3721. http://dx.doi.org/10.1242/jcs.03085.
40. **Ohno H.** 2006. Physiological roles of clathrin adaptor AP complexes: lessons from mutant animals. J Biochem **139:**943–948. http://dx.doi.org/10.1093/jb/mvj120.
41. **Szymkiewicz I, Shupliakov O, Dikic I.** 2004. Cargo- and compartment-selective endocytic scaffold proteins. Biochem J **383:**1–11. http://dx.doi.org/10.1042/BJ20040913.
42. **Schiavo G, Greensmith L, Hafezparast M, Fisher EM.** 2013. Cytoplasmic dynein heavy chain: the servant of many masters. Trends Neurosci **36:**641–651. http://dx.doi.org/10.1016/j.tins.2013.08.001.
43. **Ninkovic M, Mitkovski M, Kohl T, Stuhmer W, Pardo LA.** 2012. Physical and functional interaction of KV10.1 with Rabaptin-5 impacts ion channel trafficking. FEBS Lett **586:**3077–3084. http://dx.doi.org/10.1016/j.febslet.2012.07.055.
44. **Kaksonen M, Toret CP, Drubin DG.** 2006. Harnessing actin dynamics for clathrin-mediated endocytosis. Nat Rev Mol Cell Biol **7:**404–414. http://dx.doi.org/10.1038/nrm1940.
45. **Sun Y, Martin AC, Drubin DG.** 2006. Endocytic internalization in budding yeast requires coordinated actin nucleation and myosin motor activity. Dev Cell **11:**33–46. http://dx.doi.org/10.1016/j.devcel.2006.05.008.
46. **Okreglak V, Drubin DG.** 2007. Cofilin recruitment and function during actin-mediated endocytosis dictated by actin nucleotide state. J Cell Biol **178:**1251–1264. http://dx.doi.org/10.1083/jcb.200703092.
47. **McMurray MA, Stefan CJ, Wemmer M, Odorizzi G, Emr SD, Thorner J.** 2011. Genetic interactions with mutations affecting septin assembly reveal ESCRT functions in budding yeast cytokinesis. Biol Chem **392:**699–712.
48. **Mostowy S, Cossart P.** 2012. Septins: the fourth component of the cytoskeleton. Nat Rev Mol Cell Biol **13:**183–194.
49. **Engqvist-Goldstein AE, Warren RA, Kessels MM, Keen JH, Heuser J, Drubin DG.** 2001. The actin-binding protein Hip1R associates with clathrin during early stages of endocytosis and promotes clathrin assembly in vitro. J Cell Biol **154:**1209–1223. http://dx.doi.org/10.1083/jcb.200106089.
50. **Berryman M, Bretscher A.** 2000. Identification of a novel member of the chloride intracellular channel gene family (CLIC5) that associates with the actin cytoskeleton of placental microvilli. Mol Biol Cell **11:**1509–1521. http://dx.doi.org/10.1091/mbc.11.5.1509.
51. **Bannert N, Vollhardt K, Asomuddinov B, Haag M, Konig H, Norley S, Kurth R.** 2003. PDZ domain-mediated interaction of interleukin-16 precursor proteins with myosin phosphatase targeting subunits. J Biol Chem **278:**42190–42199. http://dx.doi.org/10.1074/jbc.M306669200.
52. **Nakamura H, Hori K, Tanaka-Okamoto M, Higashiyama M, Itoh Y, Inoue M, Morinaka S, Miyoshi J.** 2011. Decreased expression of LMO7 and its clinicopathological significance in human lung adenocarcinoma. Exp Ther Med **2:**1053–1057.

53. **Derijard B, Hibi M, Wu IH, Barrett T, Su B, Deng T, Karin M, Davis RJ.** 1994. JNK1: a protein kinase stimulated by UV light and Ha-Ras that binds and phosphorylates the c-Jun activation domain. Cell **76:**1025–1037. http://dx.doi.org/10.1016/0092-8674(94)90380-8.
54. **Tanoue T, Adachi M, Moriguchi T, Nishida E.** 2000. A conserved docking motif in MAP kinases common to substrates, activators and regulators. Nat Cell Biol **2:**110–116. http://dx.doi.org/10.1038/35000065.
55. **Bjorkblom B, Ostman N, Hongisto V, Komarovski V, Filen JJ, Nyman TA, Kallunki T, Courtney MJ, Coffey ET.** 2005. Constitutively active cytoplasmic c-Jun N-terminal kinase 1 is a dominant regulator of dendritic architecture: role of microtubule-associated protein 2 as an effector. J Neurosci **25:**6350–6361. http://dx.doi.org/10.1523/JNEUROSCI.1517-05.2005.
56. **Ogimoto G, Yudowski GA, Barker CJ, Kohler M, Katz AI, Feraille E, Pedemonte CH, Berggren PO, Bertorello AM.** 2000. G protein-coupled receptors regulate Na+,K+-ATPase activity and endocytosis by modulating the recruitment of adaptor protein 2 and clathrin. Proc Natl Acad Sci U S A **97:**3242–3247. http://dx.doi.org/10.1073/pnas.97.7.3242.